

Ambipolar Diffusion and Drift in Computational Weakly-Ionized Plasmadynamics

Bernard Parent*, Sergey O. Macheret[†] and Mikhail N. Shneider[‡]

Modeling of ambipolar diffusion and drift taking place within a weakly-ionized fluid can lead to some convergence difficulties when the ion conservation equation and the electric field potential equation are solved consecutively. A novel formulation of the ion flow rate is proposed here that reduces the computing effort to reach convergence by a factor of 10 or more. It is shown that by recasting the ion flow rate in terms of drift and ambipolar diffusion components, the sensitivity to the electric field is reduced hence alleviating the stiffness of the system of equations and permitting significantly faster convergence. What makes the method particularly appealing is that (i) it yields faster convergence without affecting the accuracy of the converged solution and (ii) it is not restricted to specific discretization or relaxation schemes and can hence be readily implemented in existing flow solvers. Because it is developed in general form (*i.e.* applicable to a multicomponent plasma in the simultaneous presence of electric current and magnetic and electric fields), the method is notably well-suited to simulate ambipolar diffusion within ionized multi-species flow solvers and is recommended for all flowfields as long as the plasma remains weakly-ionized and quasi-neutral.

1. Introduction

AMBIPOLAR diffusion is a phenomenon that occurs within a plasma when a spatial gradient of the number density of at least one of the charged species is present. The phenomenon is caused by the different charged species having different diffusivities, hence resulting in some of the charged species diffusing more or less rapidly than the others, which would lead to a loss of neutrality of the plasma. A minor loss of neutrality, however, induces an ambipolar electric field which, if the Debye length is sufficiently small, slows down the fast-diffusing species and speeds up the slow-diffusing species in such a way that the plasma remains quasi-neutral.

For a non-magnetized plasma composed of electrons and only one type of positive ions, a straightforward derivation shows that the effect of the ambipolar electric field causes the diffusion coefficient of the ions to be augmented according to the following expression (see for instance Ref. [1, p. 187]):

$$D_a = \left(1 + \frac{T_e}{T_i}\right) D_i \quad (1)$$

where D_i is the molecular diffusivity of the ions in the neutrals, D_a is the ambipolar diffusion coefficient, T_e is the electron temperature, and T_i is the temperature of the ions. From the latter, it is apparent that ambipolar diffusion effects would be particularly important when the plasma is in thermal non-equilibrium (that is, when the electron temperature differs significantly from the bulk gas temperature). Significant thermal non-equilibrium is a common feature of weakly-ionized plasmas under strong applied electromagnetic fields. For instance, in plasma aerodynamics [2, 3, 4] and in airborne MHD power generation [5] or MHD acceleration [6], it is not uncommon for the electron temperature to reach values in excess of 20,000 K while the bulk gas temperature remains at 300-600 K. For such applications, the ambipolar diffusion coefficient would be almost 100 times greater than the molecular diffusion coefficient, and would approach or even exceed the turbulence eddy diffusion coefficient.

*Faculty Member, Dept. of Aerospace Engineering, Pusan National University, Busan 609-735, Korea, <http://www.bernardparent.com>.

[†]Senior Research Scientist, Dept. of Mechanical and Aerospace Engineering, Princeton University, Princeton, NJ 08544-5263, USA. Current address: Lockheed Martin Aeronautics Company, 1011 Lockheed Way, Palmdale, California 93599-0160.

[‡]Senior Research Scientist, Dept. of Mechanical and Aerospace Engineering, Princeton University, Princeton, NJ 08544-5263, USA.

It follows that, in order to properly predict weakly-ionized flowfields under strong applied fields, ambipolar diffusion effects should be modeled as accurately as possible.

The simple expression presented in Eq. (1) is not appropriate for ambipolar diffusion occurring in many weakly-ionized plasmas because (i) it is limited to a plasma consisting of electrons and one type of positive ions, while weakly-ionized plasmas in air and many other gases have more than one type of positive ions and also contain various types of negative ions, and (ii) it is valid only for plasmas under no applied magnetic field. Ambipolar diffusion models for a four-component plasma (one type of positive ions, one type of negative ions, and electrons) were proposed by Thompson [7] and by Oskam [8]. The four-component ambipolar model by Thompson was further generalized by Suslov and Tiskii [9] and independently by Rogoff [10] and by Ramshaw and Chang [11, 12] to plasmas with any number of ion species. While the latter models are general enough to be applicable to a multicomponent plasma, including those with negative ions, they cannot be applied to cases in which a significant induced or external magnetic field is present.

When under the influence of a magnetic field, the ambipolar diffusion in a three-component plasma (one type of positive ions, electrons, and neutrals) can be readily derived to be equal to (see for instance Refs. [13, 14, 15], and Ref. [1, p. 189]):

$$D_a = \left(1 + \frac{T_e}{T_i}\right) \frac{D_i}{1 + \mu_e \mu_i B_\perp^2} \quad (2)$$

where B_\perp is the component of the magnetic field vector perpendicular to the diffusion velocity, μ_e is the electron mobility, and μ_i is the ion mobility. However, the latter cannot be applied to a plasma having negative ions or several types of positive ions with different mobilities. In Refs. [16, 17, 18], and more recently [19, 20, 21], several theories were proposed to overcome this limitation. Despite an in-depth theoretical treatment of the physical processes, the latter studies came short of yielding a general expression for the ion flow rate that is (i) applicable to a multicomponent magnetized plasma, and (ii) that can be used in the general case independently of the electric field, magnetic field, or current distribution.

Such a general expression for the ion flow rate was rather first proposed by Ramshaw and Chang [22] and dubbed the SCEBD model (Self-Consistent Effective Binary Diffusion Approximation). The SCEBD model is, however, limited to a two-temperature plasma in which all the ions share the same temperature as the neutrals, and also uses approximate weighting factors. To improve the model, Ramshaw and Chang subsequently recommended more accurate approximations to the weighting factors in Refs. [23, 24]. Another substantial drawback of the SCEBD scheme is its lack of robustness at strong magnetic field. When the magnetic field is very strong, the scheme has been observed to be difficult to integrate and to result in erratic convergence behavior due to the strong coupling of the ambipolar diffusion terms with the electric and magnetic fields [25].

The objective of this paper is to develop a numerical method that would enable accurate modeling of ambipolar diffusion and drift phenomena in quasi-neutral plasmas in the general case (that is, in the presence of current, electric field, and magnetic field). Specifically, a newly recast expression for the ion flow rate is derived. This expression is generally valid for a multicomponent magnetoplasma and overcomes the shortcomings of SCEBD. Indeed, we will show that it is possible to recast the ion flow rate in terms of drift and ambipolar diffusion terms while not introducing approximate weighting factors or making other approximations. Furthermore, because the recast form of the ion flow rate proposed herein is not as strongly dependent on the electric field, the coupling with the potential equation is weakened. This results in a more robust numerical method that yields significantly faster convergence.

This paper is structured as follows. First, the physical model is presented. Second, we derive a recast form of the ion conservation equation that is applicable to a multicomponent plasma in the general case and that is amenable to integration. Third, several test cases are solved in 1D and 2D using the proposed method, and an assessment is made of the effect of a strong electric field and magnetic field on the performance of the method.

2. Physical Model

While the recast form of the ion conservation equation that is presented herein is intended to be used in CFD codes in which the neutrals momentum, energy, and mass conservation equations are solved, the physical model is here limited for ease of reproducibility to the charged species conservation equations and the electric field potential equation, with the neutrals properties being set to a constant throughout the domain.

2.1. Charged Species Conservation Equation

For a multicomponent plasma, it is necessary to solve a separate conservation equation for each type of charged species:

$$\frac{\partial N_k}{\partial t} + \sum_{i=1}^3 \frac{\partial}{\partial x_i} (N_k \mathbf{V}_i^k) = W_k \quad (3)$$

where N_k is the number density, W_k represents the sources and sinks (*e.g.* due to ionization, recombination, attachment, and detachment), and \mathbf{V}^k the charged species velocity including both drift and diffusion. The charged species velocity can be obtained from the momentum equation.

2.2. Charged Species Momentum Equation

For a weakly-ionized plasma, the momentum equation simplifies to:

$$\mathbf{V}^k = \mathbf{V}^n + s_k \mu_k (\mathbf{E} + \mathbf{V}^k \times \mathbf{B}) - \frac{\mu_k}{|C_k| N_k} \nabla P_k \quad (4)$$

where s_k is the sign of the charge (-1 for electrons, -1 for negative ions, $+1$ for positive ions), C_k is the charge ($-e$ for the electrons, $-2e$ for the doubly-charged negative ions, $+e$ for the singly-charged positive ions, *etc.*), \mathbf{V}^n is the velocity of the neutrals including drift and diffusion, μ_k the species mobility, ∇P_k is the pressure gradient, \mathbf{E} is the electric field, and \mathbf{B} is the magnetic field. In deriving Eq. (4), it was assumed that the shear stresses, the collisional forces between charged species, and the inertia change are negligible compared to the collisional forces between the charged species and the neutrals. These assumptions can be shown to be well justified as long as the plasma remains weakly-ionized.

Then, should the tensor mobility matrix $\tilde{\mu}^k$ be defined as:

$$\tilde{\mu}^k \equiv \frac{\mu_k}{1 + \mu_k^2 |\mathbf{B}|^2} \begin{bmatrix} 1 + \mu_k^2 B_1^2 & \mu_k^2 B_1 B_2 + s_k \mu_k B_3 & \mu_k^2 B_1 B_3 - s_k \mu_k B_2 \\ \mu_k^2 B_1 B_2 - s_k \mu_k B_3 & 1 + \mu_k^2 B_2^2 & \mu_k^2 B_2 B_3 + s_k \mu_k B_1 \\ \mu_k^2 B_1 B_3 + s_k \mu_k B_2 & \mu_k^2 B_2 B_3 - s_k \mu_k B_1 & 1 + \mu_k^2 B_3^2 \end{bmatrix} \quad (5)$$

we can rewrite the charged species velocity in tensor form as follows:

$$\mathbf{V}_i^k = \mathbf{V}_i^n + \sum_{j=1}^3 s_k \tilde{\mu}_{ij}^k (\mathbf{E} + \mathbf{V}^n \times \mathbf{B})_j - \sum_{j=1}^3 \frac{\tilde{\mu}_{ij}^k}{|C_k| N_k} \frac{\partial P_k}{\partial x_j} \quad (6)$$

The latter equation can be used to obtain the velocity (including drift and diffusion) of singly-charged positive ions, singly-charged negative ions, electrons, doubly-charged negative/positive ions, *etc.*

2.3. Electric Field Potential Equation

In order to close the system of equations, an expression for the electric field must be determined. Such expression can be found from the current continuity equation:

$$\sum_{i=1}^3 \frac{\partial \mathbf{J}_i}{\partial x_i} = 0 \quad (7)$$

with the current defined as:

$$\mathbf{J}_i \equiv \sum_{k=1}^{n_s} C_k N_k \mathbf{V}_i^k \quad (8)$$

with n_s the number of charged species including electrons. After substituting the charged species velocity shown in Eq. (6) in the latter, rewriting the pressure in terms of the temperature and number density through the ideal gas law $P_k = N_k k_B T_k$, and assuming a quasi-neutral plasma, the current becomes:

$$\mathbf{J}_i = \underbrace{\sum_{k=1}^{n_s} \sum_{j=1}^3 \tilde{\mu}_{ij}^k |C_k| N_k (\mathbf{E} + \mathbf{V}^n \times \mathbf{B})_j}_{\text{current due to the electric field in the neutrals reference frame}} - \underbrace{\sum_{k=1}^{n_s} \sum_{j=1}^3 s_k \tilde{\mu}_{ij}^k N_k k_B \frac{\partial T_k}{\partial x_j}}_{\text{current due to thermal diffusion of the charged species}} - \underbrace{\sum_{k=1}^{n_s} \sum_{j=1}^3 s_k \tilde{\mu}_{ij}^k k_B T_k \frac{\partial N_k}{\partial x_j}}_{\text{current due to the mass diffusion of the charged species}} \quad (9)$$

Then, after substituting Eq. (9) into the current continuity equation (7), and defining the potential such that $\mathbf{E} = -\nabla\phi$, the electric field potential equation can be found:

$$\sum_{i=1}^3 \frac{\partial}{\partial x_i} \sum_{j=1}^3 \tilde{\sigma}_{ij} \left(-\frac{\partial \phi}{\partial x_j} + (\mathbf{V}^n \times \mathbf{B})_j \right) = \sum_{i=1}^3 \frac{\partial}{\partial x_i} \sum_{j=1}^3 \sum_{k=1}^{n_s} s_k \tilde{\mu}_{ij}^k \frac{\partial P_k}{\partial x_j} \quad (10)$$

with the tensor conductivity $\tilde{\sigma}$ equal to:

$$\tilde{\sigma}_{ij} = \sum_{k=1}^{n_s} \tilde{\mu}_{ij}^k |C_k| N_k \quad (11)$$

This variant of the electric field potential equation includes the ion slip for each type of ion.

2.4. Neutrality Condition

For a neutral plasma, the solution of the potential equation (and hence, the current continuity equation) and of all ion conservation equations ensures that the electron conservation equation is satisfied provided that the electron number density is determined through the neutrality condition:

$$N_e = \frac{1}{|C_e|} \sum_{k=1}^{n_i} C_k N_k \quad (12)$$

where n_i is the number of ion species in the plasma.

2.5. Dielectric Boundary Condition

Since the number of neutrals absorbed at the surface is at quasi-steady-state, the gas-phase neutrals reflect entirely off a dielectric surface, and the gradient of the neutrals number density at the boundary vanishes:

$$\frac{\partial N_n}{\partial \eta} = 0 \quad (13)$$

with η a coordinate perpendicular to the dielectric boundary. The same boundary condition does not hold for ions, however. Indeed, ions can not reflect off a dielectric because of the relatively large number of electrons attached to the surface resulting in a very fast recombination rate on the surface itself. Because of this effect, all ions reaching the dielectric effectively get transformed into neutrals and “disappear”. The recombination of the ions with the electrons takes place within the non-neutral region of the plasma sheath located within a few Debye lengths of the dielectric. In this paper, the non-neutral region of the sheath is not resolved. Rather, we assume the non-neutral sheath to be of negligible thickness and set the ion and electron number densities to zero at the boundary:

$$N_e = 0 \quad \text{and} \quad N_i = 0 \quad (14)$$

The latter assumes that the ion flux from the sheath to the adjacent quasi-neutral plasma is zero. This is a commonly accepted and reasonable assumption as long as the sheath is thin and the electric field within the sheath does not result in a significant amount of Townsend (*i.e.* electron-impact) ionization. Further assuming that there is no secondary emission from the surface, no current can flow transverse to the dielectric (this condition is commonly referred to as the electrically floating surface condition). Therefore, the component of the current vector perpendicular to the surface is here set to zero:

$$\mathbf{J}_\eta = 0 \quad (15)$$

with η the coordinate perpendicular to the dielectric.

3. Recast of the Potential Equation

As was shown in Ref. [26], the discretization of Eq. (10) using centered stencils can lead to some spurious oscillations when the Hall parameter is high and when a gradient of the conductivity is present. It is recalled that in a plasma, the Hall parameter β_e corresponds to the product between the electron mobility and the magnitude of the magnetic field, *i.e.* $\beta_e = \mu_e |\mathbf{B}|$. Because ambipolar diffusion necessarily entails a conductivity gradient, spurious oscillations could occur when the magnetic field becomes substantial. The appearance of spurious oscillations is due to some of the cross-diffusion terms within the potential

equation being essentially convection derivatives and requiring upwinding. We can overcome this difficulty by writing the tensorial conductivity in terms of a symmetric and a skew-symmetric part:

$$\tilde{\sigma} = \tilde{\sigma}^s + \tilde{\sigma}^{ss} \quad (16)$$

with the symmetric part of the tensor conductivity equal to:

$$\tilde{\sigma}^s = \sum_{k=1}^{n_s} \frac{\mu_k |C_k| N_k}{1 + \mu_k^2 |B|^2} \begin{bmatrix} 1 + \mu_k^2 B_1^2 & \mu_k^2 B_1 B_2 & \mu_k^2 B_1 B_3 \\ \mu_k^2 B_1 B_2 & 1 + \mu_k^2 B_2^2 & \mu_k^2 B_2 B_3 \\ \mu_k^2 B_1 B_3 & \mu_k^2 B_2 B_3 & 1 + \mu_k^2 B_3^2 \end{bmatrix} \quad (17)$$

and the skew-symmetric part of the tensor conductivity equal to:

$$\tilde{\sigma}^{ss} = \sum_{k=1}^{n_s} \frac{\mu_k |C_k| N_k}{1 + \mu_k^2 |B|^2} \begin{bmatrix} 0 & s_k \mu_k B_3 & -s_k \mu_k B_2 \\ -s_k \mu_k B_3 & 0 & s_k \mu_k B_1 \\ s_k \mu_k B_2 & -s_k \mu_k B_1 & 0 \end{bmatrix} \quad (18)$$

Then, should we define the skew-symmetric wave speed as:

$$a_i^{ss} \equiv - \sum_{j=1}^3 \frac{\partial \tilde{\sigma}_{ji}^{ss}}{\partial x_j} \quad (19)$$

It can be shown that the potential equation becomes exactly [26]:

$$\sum_{i=1}^3 \frac{\partial}{\partial x_i} a_i^{ss} \phi - \sum_{i=1}^3 \frac{\partial}{\partial x_i} \sum_{j=1}^3 \tilde{\sigma}_{ij}^s \frac{\partial \phi}{\partial x_j} = \sum_{i=1}^3 \frac{\partial}{\partial x_i} \sum_{j=1}^3 \left(-\tilde{\sigma}_{ij} (V^n \times B)_j + \sum_{k=1}^{n_s} s_k \tilde{\mu}_{ij}^k \frac{\partial P_k}{\partial x_j} \right) \quad (20)$$

It is emphasized that the recast form of the potential outlined in Eq. (20) is equivalent to the standard form outlined in Eq. (10). That is, the physical model is not altered. However, the recast form of the potential equation is better suited for discretization because the skew-symmetric cross-diffusion terms are written as convection derivatives which can be discretized using upwinded stencils. Because the cross-diffusion terms are prevalent within ambipolar diffusion problems in the presence of a magnetic field, using the recast form of the potential equation is crucial to guarantee a monotonic solution free of nonphysical oscillations.

4. Novel Recast of the Ion Conservation Equation

The ion conservation equation as it is written in Eq. (3) leads to severe convergence difficulties if solved in conjunction with the electric field potential equation using a discrete method. The convergence problems originate from the ion conservation equation being too strongly dependent on the electric field. For many problems (such as those shown subsequently in Section 6), the stiffness of the system of discrete equations is such that convergence to steady-state requires tens of thousands of iterations. For other problem setups, it may even be impossible to obtain a solution.

To alleviate the stiffness of the system of equations, the ion conservation equation needs to be recast in a form that is not as strongly dependent on the electric field. For this purpose, a new approach is proposed here. The proposed method consists of first splitting the electric field as a sum of \mathbf{E}' and \mathbf{E}'' vectors with the \mathbf{E}' vector defined as the component of the electric field responsible for suppressing the current originating from mass diffusion of the charged species (see current components in Eq. (9) above):

$$\sum_{k=1}^{n_s} \sum_{j=1}^3 \tilde{\mu}_{ij}^k |C_k| N_k \mathbf{E}'_j \equiv \sum_{k=1}^{n_s} \sum_{j=1}^3 s_k \tilde{\mu}_{ij}^k k_B T_k \frac{\partial N_k}{\partial x_j} \quad (21)$$

and with the vector \mathbf{E}'' defined such that the sum of \mathbf{E}' and \mathbf{E}'' yields the electric field:

$$\mathbf{E}'' \equiv \mathbf{E} - \mathbf{E}' \quad (22)$$

The equation for \mathbf{E}' can also be written in matrix form:

$$\begin{bmatrix} Z_{11} & Z_{12} & Z_{13} \\ Z_{21} & Z_{22} & Z_{23} \\ Z_{31} & Z_{32} & Z_{33} \end{bmatrix}^{-1} \begin{bmatrix} \mathbf{E}'_1 \\ \mathbf{E}'_2 \\ \mathbf{E}'_3 \end{bmatrix} = \sum_{k=1}^{n_s} \sum_{j=1}^3 \begin{bmatrix} s_k \tilde{\mu}_{1j}^k k_B T_k \partial N_k / \partial x_j \\ s_k \tilde{\mu}_{2j}^k k_B T_k \partial N_k / \partial x_j \\ s_k \tilde{\mu}_{3j}^k k_B T_k \partial N_k / \partial x_j \end{bmatrix} \quad (23)$$

with the matrix Z equal to:

$$Z = \left[\sum_{k=1}^{n_s} \tilde{\mu}^k |C_k| N_k \right]^{-1} \quad (24)$$

Making use of the neutrality condition, Eq. (12), the matrix Z can be expressed in such a way that it does not depend on the electron number density:

$$Z = \left[\sum_{k=1}^{n_i} (\tilde{\mu}^e + s_k \tilde{\mu}^k) C_k N_k \right]^{-1} \quad (25)$$

where n_i stands for the number of ion species in the plasma. After multiplying Eq. (23) on both sides by Z we get:

$$\begin{bmatrix} \mathbf{E}'_1 \\ \mathbf{E}'_2 \\ \mathbf{E}'_3 \end{bmatrix} = \sum_{k=1}^{n_s} \sum_{j=1}^3 \begin{bmatrix} Z_{11} & Z_{12} & Z_{13} \\ Z_{21} & Z_{22} & Z_{23} \\ Z_{31} & Z_{32} & Z_{33} \end{bmatrix} \begin{bmatrix} s_k \tilde{\mu}_{1j}^k k_B T_k \partial N_k / \partial x_j \\ s_k \tilde{\mu}_{2j}^k k_B T_k \partial N_k / \partial x_j \\ s_k \tilde{\mu}_{3j}^k k_B T_k \partial N_k / \partial x_j \end{bmatrix} \quad (26)$$

We can rewrite this equation back in tensor form:

$$\mathbf{E}'_m = \sum_{n=1}^3 \sum_{k=1}^{n_s} \sum_{j=1}^3 Z_{mn} s_k \tilde{\mu}_{nj}^k k_B T_k \frac{\partial N_k}{\partial x_j} \quad (27)$$

Then, for convenience, exchange the m index for the j index, and also exchange the k index for the r index. Then, the \mathbf{E}' vector becomes:

$$\mathbf{E}'_j = \sum_{n=1}^3 \sum_{r=1}^{n_s} \sum_{m=1}^3 Z_{jn} s_r \tilde{\mu}_{nm}^r k_B T_r \frac{\partial N_r}{\partial x_m} \quad (28)$$

Having found an expression for the \mathbf{E}' vector, we now proceed to express the ion flow rate in terms of drift and diffusion components. To do so, we express the ion velocity using Eq. (6) and note that $\mathbf{E} = \mathbf{E}' + \mathbf{E}''$:

$$N_k \mathbf{V}_i^k = N_k \mathbf{V}_i^n + \sum_{j=1}^3 s_k \tilde{\mu}_{ij}^k N_k (\mathbf{E}' + \mathbf{E}'' + \mathbf{V}^n \times \mathbf{B})_j - \sum_{j=1}^3 \frac{\tilde{\mu}_{ij}^k}{|C_k|} \frac{\partial P_k}{\partial x_j} \quad (29)$$

Then, we substitute the \mathbf{E}' vector obtained in Eq. (28) in the latter and expand the pressure gradient term using the ideal gas law $P_k = N_k k_B T_k$:

$$\begin{aligned} N_k \mathbf{V}_i^k &= N_k \mathbf{V}_i^n + \sum_{j=1}^3 s_k \tilde{\mu}_{ij}^k N_k (\mathbf{E}'' + \mathbf{V}^n \times \mathbf{B})_j - \sum_{j=1}^3 \frac{\tilde{\mu}_{ij}^k N_k k_B}{|C_k|} \frac{\partial T_k}{\partial x_j} - \sum_{j=1}^3 \frac{\tilde{\mu}_{ij}^k k_B T_k}{|C_k|} \frac{\partial N_k}{\partial x_j} \\ &+ \sum_{j=1}^3 s_k \tilde{\mu}_{ij}^k N_k \sum_{n=1}^3 \sum_{r=1}^{n_s} \sum_{m=1}^3 Z_{jn} s_r \tilde{\mu}_{nm}^r k_B T_r \frac{\partial N_r}{\partial x_m} \end{aligned} \quad (30)$$

Then, for convenience, exchange the m index for the j index in the last term on the RHS, and take the electrons out of the sum:

$$\begin{aligned} N_k \mathbf{V}_i^k &= N_k \mathbf{V}_i^n + \sum_{j=1}^3 s_k \tilde{\mu}_{ij}^k N_k (\mathbf{E}'' + \mathbf{V}^n \times \mathbf{B})_j - \sum_{j=1}^3 \frac{\tilde{\mu}_{ij}^k N_k k_B}{|C_k|} \frac{\partial T_k}{\partial x_j} - \sum_{j=1}^3 \frac{\tilde{\mu}_{ij}^k k_B T_k}{|C_k|} \frac{\partial N_k}{\partial x_j} \\ &+ \sum_{m=1}^3 s_k \tilde{\mu}_{im}^k N_k \sum_{n=1}^3 \sum_{r=1}^{n_i} \sum_{j=1}^3 Z_{mn} s_r \tilde{\mu}_{nj}^r k_B T_r \frac{\partial N_r}{\partial x_j} - \sum_{m=1}^3 s_k \tilde{\mu}_{im}^k N_k \sum_{n=1}^3 \sum_{j=1}^3 Z_{mn} \tilde{\mu}_{nj}^e k_B T_e \frac{\partial N_e}{\partial x_j} \end{aligned} \quad (31)$$

Then express the electron number density using the neutrality condition, Eq. (12), and note that $C_r = s_r |C_r|$:

$$\begin{aligned} N_k \mathbf{V}_i^k &= N_k \mathbf{V}_i^n + \sum_{j=1}^3 s_k \tilde{\mu}_{ij}^k N_k (\mathbf{E}'' + \mathbf{V}^n \times \mathbf{B})_j - \sum_{j=1}^3 \frac{\tilde{\mu}_{ij}^k N_k k_B}{|C_k|} \frac{\partial T_k}{\partial x_j} - \sum_{j=1}^3 \frac{\tilde{\mu}_{ij}^k k_B T_k}{|C_k|} \frac{\partial N_k}{\partial x_j} \\ &+ \sum_{m=1}^3 s_k \tilde{\mu}_{im}^k N_k \sum_{n=1}^3 \sum_{r=1}^{n_i} \sum_{j=1}^3 Z_{mn} s_r \tilde{\mu}_{nj}^r k_B T_r \frac{\partial N_r}{\partial x_j} - \sum_{m=1}^3 s_k \tilde{\mu}_{im}^k N_k \sum_{n=1}^3 \sum_{r=1}^{n_i} \sum_{j=1}^3 Z_{mn} s_r \tilde{\mu}_{nj}^e k_B T_e \frac{|C_r|}{|C_e|} \frac{\partial N_r}{\partial x_j} \end{aligned} \quad (32)$$

The latter can be written in compact form as:

$$N_k \mathbf{V}_i^k = N_k \mathbf{v}_i^k - \sum_{j=1}^3 \sum_{r=1}^{n_i} D_{ij}^{kr} \frac{\partial N_r}{\partial x_j} \quad (33)$$

where \mathbf{v}^k is the drift velocity, which is here defined as the component of the velocity excluding the contributions from mass diffusion and the \mathbf{E}' component of the electric field:

$$\mathbf{v}_i^k \equiv \mathbf{V}_i^n + \sum_{j=1}^3 s_k \tilde{\mu}_{ij}^k (\mathbf{E}'' + \mathbf{V}^n \times \mathbf{B})_j - \sum_{j=1}^3 \frac{\tilde{\mu}_{ij}^k k_B}{|C_k|} \frac{\partial T_k}{\partial x_j} \quad (34)$$

and where D_{ij}^{kr} is the diffusion tensor defined as:

$$D_{ij}^{kr} \equiv \delta_{rk} \frac{k_B T_k}{|C_k|} \tilde{\mu}_{ij}^k + \sum_{m=1}^3 \sum_{n=1}^3 s_r s_k \tilde{\mu}_{im}^k N_k Z_{mn} k_B \left(\frac{|C_r|}{|C_e|} T_e \tilde{\mu}_{nj}^e - T_r \tilde{\mu}_{nj}^r \right) \quad (35)$$

where δ_{rk} is the Kronecker delta. Note that the flow rate obtained in Eq. (33) is valid only for the ions, and cannot be used for the electrons. Additionally, it is only valid in the limit of a neutral plasma.

Making use of the ion flow rate of Eq. (33), the ion conservation equation, Eq. (3), can be recast as a function of drift and diffusion terms:

$$\frac{\partial N_k}{\partial t} + \sum_{i=1}^3 \frac{\partial}{\partial x_i} (N_k \mathbf{v}_i^k) - \sum_{i=1}^3 \frac{\partial}{\partial x_i} \left(\sum_{j=1}^3 \sum_{r=1}^{n_i} D_{ij}^{kr} \frac{\partial N_r}{\partial x_j} \right) = W_k \quad (36)$$

where the drift velocity \mathbf{v} can be found from Eq. (34) and the ambipolar diffusion tensor D from Eq. (35). For a three-component plasma, the ambipolar diffusion tensor becomes a scalar due to only one type of ion being present. Further, for a three-component plasma in the absence of a magnetic field, it can be shown that the diffusion tensor outlined in Eq. (35) collapses to the well known ambipolar diffusion coefficient outlined in Eq. (1). However, when the plasma has more than three components, the diffusion of each ion species is dependent on the diffusion of the other ion species. This is why the ion flow rate shown in Eq. (33) depends on density gradients of other types of ions.

It is emphasized that Eq. (36) corresponds *exactly* to Eq. (3) in the limit of a neutral plasma, and does not therefore alter the physical model. The reason why Eq. (3) is rewritten as a sum of a drift and a diffusion component as is done above is to make the numerical method more stable. Because the diffusion tensor in Eq. (35) includes ambipolar diffusion terms and because it is free of the electric field, the ion conservation equation does not depend as strongly on the solution of the potential equation. This effectively results in less stiffly coupled discrete equations that are easier to solve numerically.

The recast ion conservation equation proposed herein has some advantages compared to alternatives. For instance, in contrast to the SCEBD scheme, it does not include *ad hoc* approximate weight factors and it does not assume that the ions share the same temperature as the neutrals. Rather, it is an *exact recast* of the physical model in the limit of a neutral plasma. Moreover, the ion conservation equation proposed herein uses an ambipolar diffusion tensor which is free of the electric field. That is not the case for the SCEBD scheme which is written in such a way that the diffusion terms exhibit a strong dependence on the electric field (see Appendix A). Perhaps for this reason, numerical tests indicate that the form proposed herein converges more reliably and is better suited to tackle diffusion phenomena at both low and high Hall parameter.

5. Discretization and Integration

For both the recast potential conservation equation, Eq. (20), and the recast ion conservation equation, Eq. (36), the convection derivative is discretized using a TVD stencil with a minmod limiter [27] while the other spatial derivatives are discretized using centered stencils. Because of the use of TVD limiters, the discretization stencils are monotonicity-preserving and are second-order accurate except nearby discontinuities.

When solving time-accurate problems, the ion conservation equation is advanced in time through an explicit Euler time marching procedure. For each time step of the ion conservation equation, the potential equation is converged to sufficient accuracy using an implicit approximate factorization algorithm [28].

When solving steady-state problems, a solution of the discrete equations is obtained through pseudotime relaxation (that is, a pseudotime derivative is added to the recast potential equation and the recast ion conservation equations). The potential

$N_e = 3.5 \times 10^{17} \text{ 1/m}^3$	$N_e = 6.5 \times 10^{17} \text{ 1/m}^3$
$N_{N_2^+} = 3 \times 10^{17} \text{ 1/m}^3$	$N_{N_2^+} = 6 \times 10^{17} \text{ 1/m}^3$
$N_{O_2^-} = 1 \times 10^{17} \text{ 1/m}^3$	$N_{O_2^-} = 1.5 \times 10^{17} \text{ 1/m}^3$
$N_{O_2^+} = 1.5 \times 10^{17} \text{ 1/m}^3$	$N_{O_2^+} = 2 \times 10^{17} \text{ 1/m}^3$
$N_n = 1 \times 10^{23} \text{ 1/m}^3$	$N_n = 1 \times 10^{23} \text{ 1/m}^3$
$T_e = 3000 \text{ K}$	$T_e = 3000 \text{ K}$
$T_{\text{ions}} = 300 \text{ K}$	$T_{\text{ions}} = 300 \text{ K}$

$L = 5 \text{ mm}$

x

FIGURE 1: Initial conditions for the 1D test cases.

and ion conservation equations are advanced in pseudotime sequentially through an approximate factorization algorithm as long as the maximum residual within the domain remains higher than a user-specified convergence threshold. To improve the convergence to steady-state, a local pseudotime stepping strategy is employed. For the ion conservation equation, the local pseudotime step is set as follows:

$$(\Delta\tau)_{N_k} = \text{CFL} \times \min_{i=1}^3 \left(\frac{\Delta x_i}{a_{\text{ref}} + \max(|\mathbf{v}_i^k|^{X_i-1}, |\mathbf{v}_i^k|^{X_i}, |\mathbf{v}_i^k|^{X_i+1})} \right) \quad (37)$$

where CFL is a non-dimensional user-defined constant, where a_{ref} is a reference sound speed, and where X_i is the grid coordinate along the i th dimension. For the potential equation, the local pseudotime step is specified as follows:

$$(\Delta\tau)_\phi = L_c \times \min_{i=1}^3 \left(\frac{\Delta x_i}{\max(\tilde{\sigma}_{ii}^{X_i-1}, \tilde{\sigma}_{ii}^{X_i}, \tilde{\sigma}_{ii}^{X_i+1})} \right) \quad (38)$$

where L_c is a user-defined characteristic length scale of the computational domain.

6. Test Cases

To test the capabilities of the proposed method, several test cases are considered in which the recast form of the ion conservation equation is solved in conjunction with the potential equation. The first series of test cases consists of one-dimensional ambipolar diffusion and drift occurring in a multicomponent air plasma. The second series of test cases focuses on the effect of the magnetic field on two-dimensional ambipolar diffusion occurring in a nitrogen plasma.

6.1. One-Dimensional Ambipolar Diffusion and Drift in a Multicomponent Plasma

In this section, the accuracy of the proposed method at predicting ambipolar diffusion and drift is assessed through a comparison with a “direct numerical simulation”. The direct numerical simulation consists in solving the ion and electron conservation equations as outlined above in Eq. (3) with the electric field found from Gauss’ law.

A comparison between the proposed method and the direct solution is obtained here for the diffusion problem depicted in Fig. 1. The species are limited to electrons, neutrals, O_2^+ ions, N_2^+ ions, and O_2^- ions, and the electron temperature is set to ten times the temperature of the heavy particules. The mobilities of the positive and negative ions are found as in Refs. [29, 30] while the mobility of the electrons is taken from Ch. 21 of Ref. [31]. No external magnetic field is applied. This validation case is particularly helpful in assessing the accuracy of the proposed numerical method because of the high temperature difference between the electrons and the ions inducing a significant ambipolar diffusion. The problem is solved in 1D because in the case of a small Debye length a direct numerical solution can only be obtained within a reasonable computational time when the problem is one-dimensional. In order to solve the system of equations, it is necessary to impose boundary conditions for the number density and the electric field. The number density does not need to be altered at the boundaries because the domain is

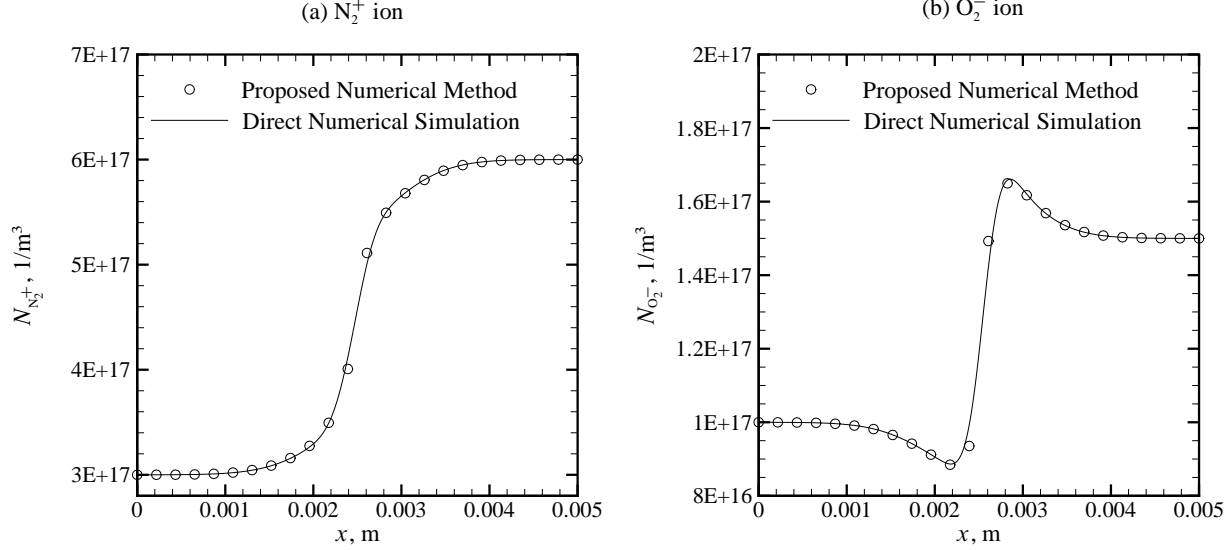


FIGURE 2. One-dimensional ambipolar diffusion in a multicomponent plasma; ion number densities at a time of 10 microseconds with the external fields set to $\mathbf{E} = 0$ and $\mathbf{B} = 0$; the grid is composed of 24 equally-spaced nodes for the proposed method and of 768 equally-spaced nodes for the direct numerical simulation.

sufficiently long so that the diffusion wave does not reach the boundary nodes. When simulating ambipolar drift, the electric field at the leftmost boundary is fixed to the external field. When simulating ambipolar diffusion, the electric field on the leftmost boundary node is continually updated according to the following expression:

$$E_x = \frac{1}{2\epsilon_0} \int_0^L \left(\sum_{k=1}^{n_s} C_k N_k \right) dx \quad (39)$$

On the rightmost boundary node, the electric field corresponds to the negative of the one on the leftmost boundary node. Fixing the electric field in this manner is necessary to guarantee no net current within the diffusion wave when performing a direct numerical simulation.

A comparison of the ion number density profiles at a time of 10 microseconds is shown in Fig. 2 for the case of no external electric field. Because no external electric field is present, ambipolar drift is negligible compared to ambipolar diffusion. It is found that the numerical method proposed herein yields ion densities in near-perfect agreement with the direct numerical simulation despite requiring a fraction of the computing effort (for equivalent accuracy, the computing effort is reduced more than 100-fold in this case). When the mesh used for the proposed method is further refined, the difference in solution between the two methods approaches zero (see grid convergence study in Table 1). This is as expected, because the relatively high density of the charged species entails a very small Debye length, which prevents significant charge separation. Because the proposed method differs from the direct solution only through the assumption of neutrality, we would indeed expect both schemes to yield essentially the same solution when the Debye length becomes very small.

A particularly interesting feature of ambipolar diffusion in the presence of negative ions is the possibility of the diffusion coefficient becoming *negative* in some regions of the plasma. This is obviously occurring in this case for the negative ions: the profile of the number density of the negative ions exhibits some local extrema, which is a consequence of the ambipolar diffusion process acting locally like a “compression”. Such a phenomenon is very well captured by the proposed method, which shows minimal error compared to the direct solution.

For the same initial conditions as the previous validation case, we now wish to assess the capabilities of the proposed method to capture ambipolar drift phenomena. Ambipolar drift refers to the increase of the effective diffusion coefficient due to a strong applied electric field. For a three-component plasma in the absence of a magnetic field, it can be shown that the effective diffusion coefficient including ambipolar diffusion and drift collapses to [32]:

$$D_{\text{eff}} = \underbrace{D_i \frac{\epsilon_0 E_{\parallel}^2}{N_e k_B T_i}}_{\text{ambipolar drift}} + \underbrace{D_i \left(1 + \frac{T_e}{T_i} \right)}_{\text{ambipolar diffusion}} \quad (40)$$

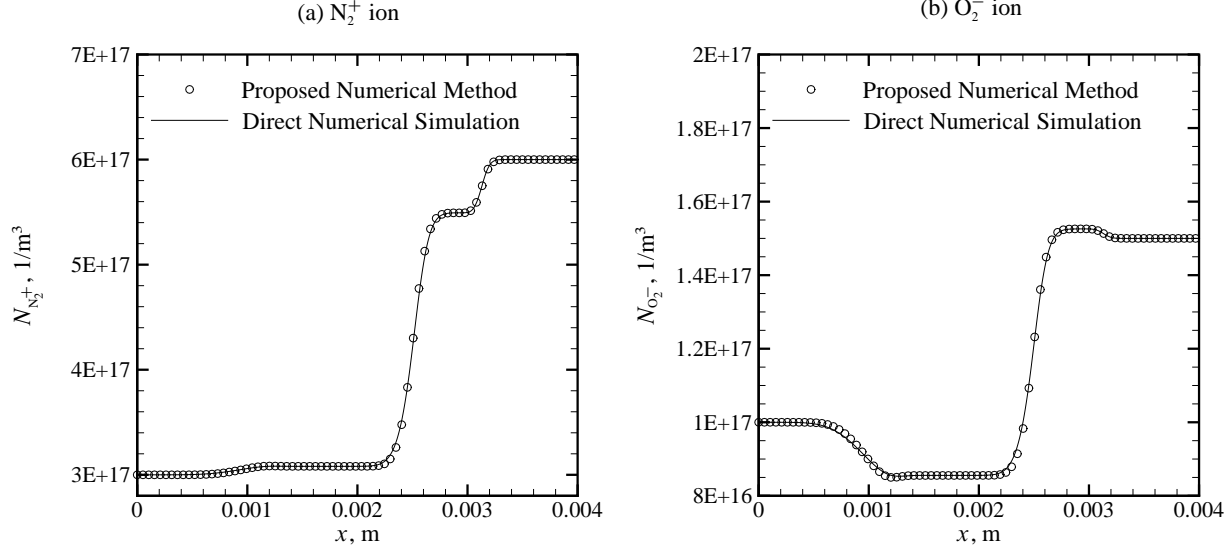


FIGURE 3. One-dimensional ambipolar drift in a multicomponent plasma; ion number densities at a time of 0.5 microsecond with the external fields set to $E_x = 40$ kV/m and $B = 0$; the grid is composed of 384 equally-spaced nodes for the proposed method and of 768 equally-spaced nodes for the direct numerical simulation (for the proposed numerical method, one in every four nodes is shown).

TABLE 1.

Assessment of relative error between the proposed method and the direct numerical simulation when solving the 1D ambipolar diffusion and ambipolar drift test cases.^{a,b,c}

Test Case	Relative error on ion number density							
	$\frac{1}{LN_{ref}} \int_0^L N_{N_2^+} - (N_{N_2^+})_{DNS} dx$				$\frac{1}{LN_{ref}} \int_0^L N_{O_2^-} - (N_{O_2^-})_{DNS} dx$			
	24 nodes	48 nodes	96 nodes	192 nodes	24 nodes	48 nodes	96 nodes	192 nodes
Ambipolar Diffusion	0.1928%	0.0470%	0.0109%	0.0029%	0.4730%	0.1092%	0.0249%	0.0067%
Ambipolar Drift	2.1291%	0.8339%	0.2982%	0.0576%	3.7309%	1.1669%	0.4300%	0.1418%

^a The reference density number N_{ref} is fixed to $\max(N_L, N_R)$ with N_L and N_R being the initial left and right states ion densities.

^b The error is measured at a time of 10 microseconds for the ambipolar test case, and at a time of 0.5 microsecond for the ambipolar drift test case.

^c The “DNS” solution is obtained with the direct method using a 768-node grid.

where $E_{||}$ is the component of the electric field parallel to the diffusion and ϵ_0 is the permittivity of free space. For ambipolar drift to play a more important role than ambipolar diffusion it can be easily shown that the electric field component parallel to the diffusion should satisfy the following condition:

$$E_{||} \gtrsim \left(\frac{N_e k_B (T_i + T_e)}{\epsilon_0} \right)^{\frac{1}{2}} \quad (41)$$

By fixing the applied electric field to 40 kV/m for the cases considered here, the latter condition is satisfied and ambipolar drift becomes as significant as ambipolar diffusion. As shown in Fig. 3, very good agreement is obtained between the proposed method and the direct numerical simulation when using a mesh made of 384 nodes. This is as anticipated, because the Debye length is small enough to guarantee the neutrality of the plasma, and when this occurs, both approaches are expected to yield the same solution. It is interesting to note that significantly more nodes are required to capture ambipolar drift compared to ambipolar diffusion (see relative error in Table 1). This is attributed to the strong external electric field increasing the coupling between the potential equation and the ion conservation equations.

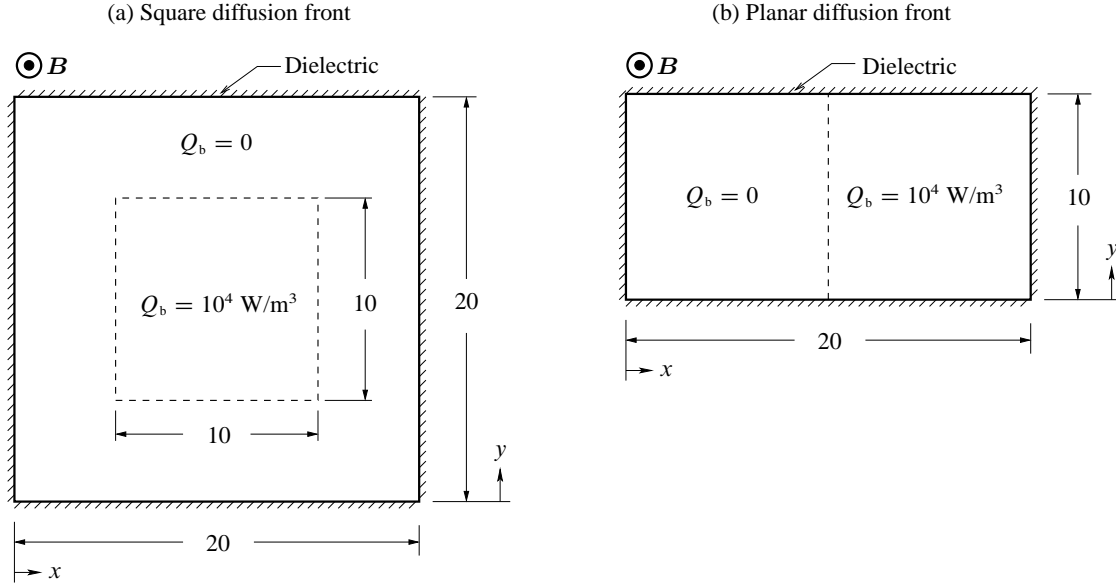


FIGURE 4. Problem setup for the two-dimensional ambipolar diffusion cases: a) square diffusion front; b) planar diffusion front. All dimensions in millimeters.

TABLE 2.
Ionization and recombination reactions taking place within the nitrogen plasma for the planar and square diffusion front cases.

No.	Reaction	Rate Coefficient ^a	Reference
1	$e^- + N_2^+ \rightarrow N_2$	$2.8 \times 10^{-7} (300/T_e)^{0.5} \text{ cm}^3/\text{s}$	[33]
2	$N_2 \rightarrow e^- + N_2^+$	$1.8 \times 10^{17} Q_b/N_{N_2} \text{ 1/s}$	[34]

^a Units: T_e in Kelvin, Q_b in W/m^3 , and N_{N_2} in $1/\text{m}^3$.

6.2. Two-Dimensional Ambipolar Diffusion in a Magnetized Plasma

We now proceed to simulate steady-state ambipolar diffusion phenomena taking place in a weakly-ionized gas in the presence of a strong magnetic field. The species present within the plasma are limited to N_2 , N_2^+ , and electrons. The nitrogen gas is ionized using externally injected electron beams with beam electron energies above 1 keV (so that the energy cost per newly produced electron-ion pair is 34 eV); the electron beam current density and thus the energy deposition rate per unit volume is uniform throughout a sharply defined area and is zero elsewhere; and it is assumed for simplicity that the only electron loss mechanism is ion-electron recombination (see the reaction rates in Table 2). The electron temperature is fixed at 8,000 K, the nitrogen temperature is set to 300 K, the nitrogen number density is set to 10^{23} 1/m^3 , the electron mobility is set to $29 \text{ m}^2/\text{Vs}$ and the ion mobility is set to $0.043 \text{ m}^2/\text{Vs}$.

As schematized in Fig. 4, two types of configurations are studied: one in which the electron beam acts on a square region in the center of the domain resulting in a square diffusion front, and another one in which the electron beam acts on the right half of the domain resulting in a “planar” diffusion front. For both types of configurations, the boundary conditions at the dielectric walls are such that the current component perpendicular to the wall is zero and the ion number density at the wall is zero. Because the ionization process is concentrated only in some areas of the domain, sharp gradients of the electron and ion number densities quickly form. Then, ambipolar diffusion takes place and spreads the ions to regions of the domain that are not ionized by the electron beam. The ion flow rate spread by ambipolar diffusion is then balanced by the rate of ion loss due to electron-ion recombination. Due to this balance between diffusion and ionization-recombination processes, a steady-state solution forms in which gradients of the ion number density are present.

The ion number density contours at different values of the magnetic induction are shown for the square front case in Fig. 5. To minimize the grid-induced error it is found necessary to use a mesh size varying between 400×400 nodes for no applied magnetic field to 800×800 nodes for the largest magnetic field considered. An analysis of the computed results reveals that the

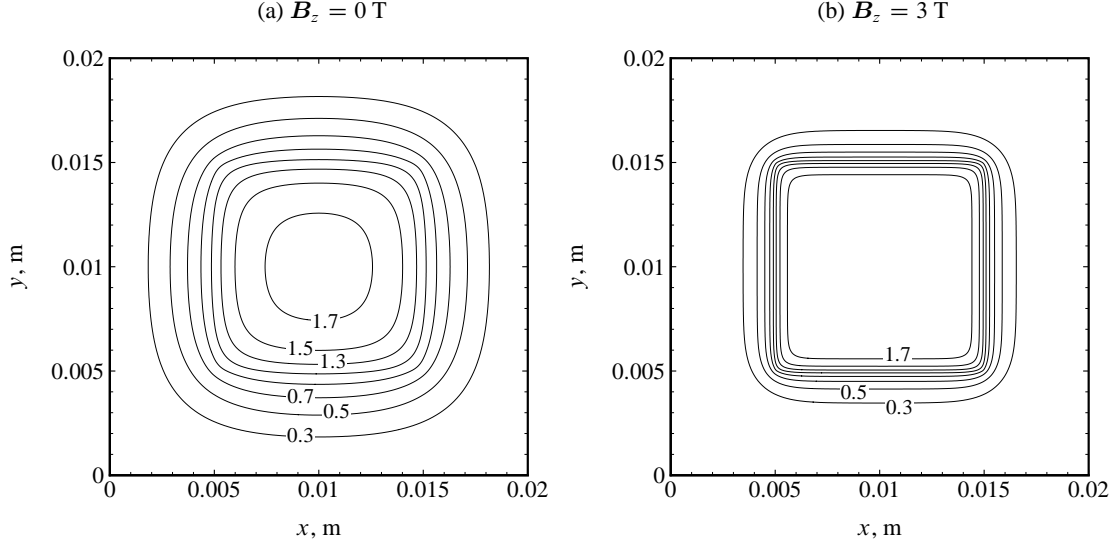


FIGURE 5. Effect of magnetic field on the nitrogen ion number density contours (in units of $10^{17}/\text{m}^3$) for the square front configuration. A mesh of 400×400 nodes is used in both cases.

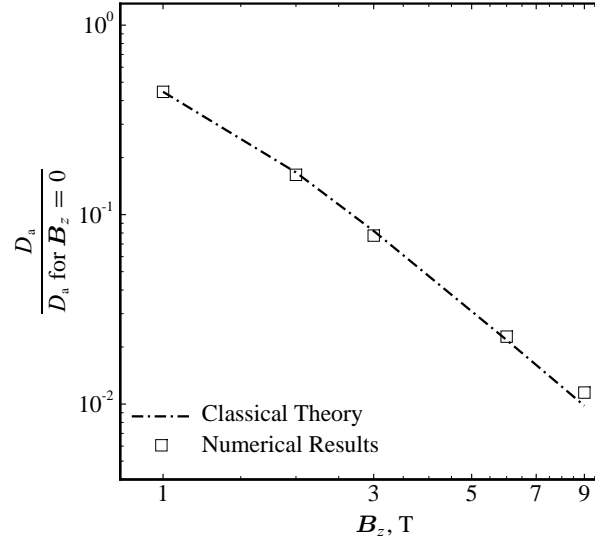


FIGURE 6: Normalized ambipolar diffusion coefficient as a function of the magnetic field for the square front configuration.

ambipolar diffusion process follows closely the classical theory. That is, the ambipolar diffusion coefficient shows a dependence on the magnetic field varying as $1/(1 + \mu_e \mu_i B_\perp^2)$, see Figure 6. This is as anticipated for such a fine mesh: because the mesh-induced error is minimized, the numerical method is expected to yield the exact solution to the physical model outlined in Section 2, and the physical model does yield the classical theory in this case because the electric field transverse to the diffusion wave is negligible (see derivation in Appendix B). This confirms the correctness of the recast form of the ion conservation equation proposed herein. Indeed, because the recast form of the ion conservation equation used to obtain the computational results corresponds to an *exact recast* of the ion conservation equation used to derive the classical theory, close agreement between the numerical results and the classical theory is expected.

A more intricate problem to solve is the “planar” configuration, in which some of the dielectric walls are located adjacent to the region ionized by the electron beam. Then, ambipolar diffusion occurs not only at the interface of the ebeam-ionized region and the non-ebeam-ionized region, but also occurs near the dielectric boundaries (see the ion density contours for the planar configuration in Fig. 7). This problem is hence particularly useful to assess the order of accuracy of the method when

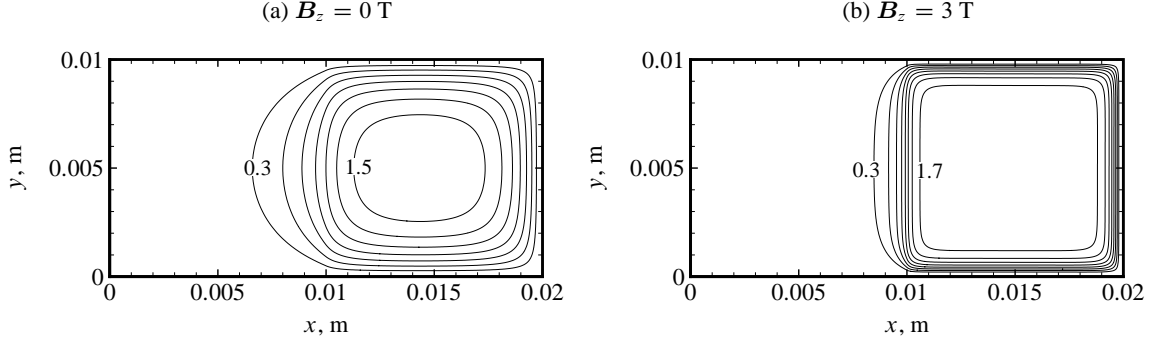


FIGURE 7. Effect of magnetic field on the nitrogen ion number density contours (in units of $10^{17}/\text{m}^3$) for the planar front configuration. A mesh of 400×200 nodes is used in both cases.

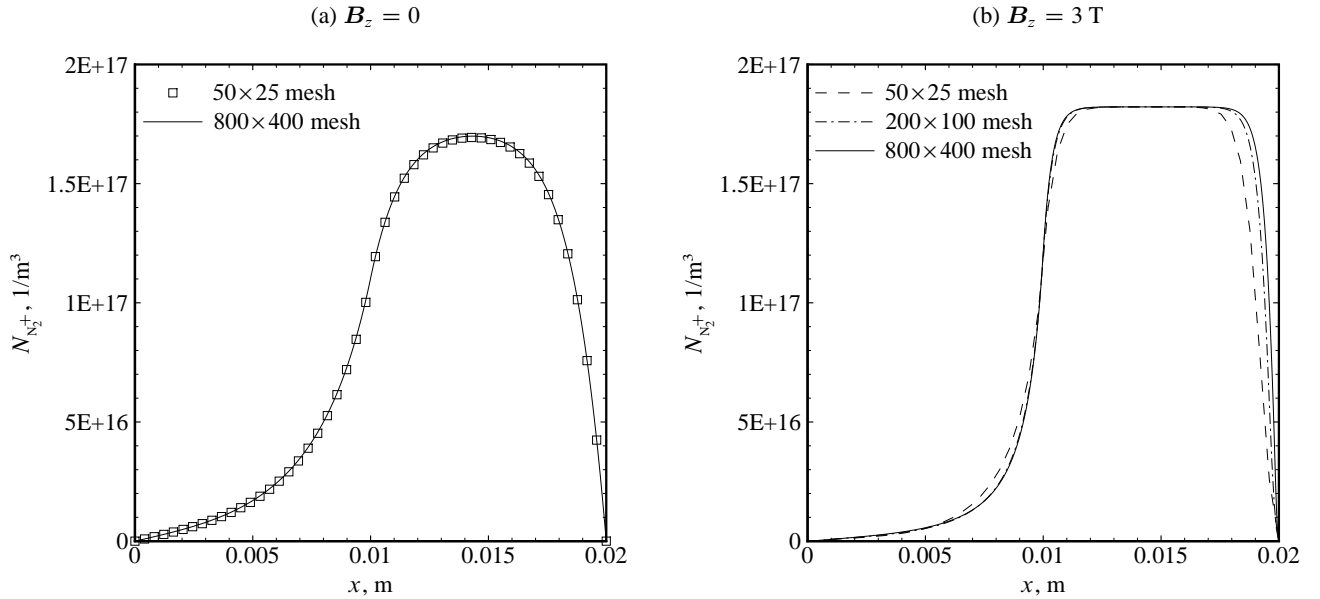


FIGURE 8: Grid convergence study of the nitrogen ion number density at $y = 5 \text{ mm}$ for the planar front configuration.

simulating ambipolar diffusion occurring both far and close to the dielectric boundary. As shown in Fig. 8, when the applied magnetic field is zero there is no discernible difference between the results obtained with the coarsest and finest meshes. The numerical results obtained with the coarsest mesh can hence be considered to be essentially free of grid-induced error in the absence of a magnetic field. On the other hand, significantly more nodes are necessary to achieve the same level of accuracy in the presence of a strong magnetic field. This is verified not to be caused by a decrease in the order of accuracy of the method. In fact, a comparison of the ion number density obtained using different meshes reveals that the order of accuracy is close to 2 whether or not a strong magnetic field is present.

The decreased performance of the method for a strong magnetic field is rather due to the latter increasing the coupling between the potential equation and the recast ion conservation equation. It is emphasized that the recast form of the ion conservation equation and the electric field potential do not depend significantly on each other when both the applied magnetic field and the applied electric field are negligible. However, when a strong magnetic field is present, there is a significant coupling between the ion conservation equation and the potential equation which results in more numerical error in the converged solution. The amount of coupling can be monitored through the vector \mathbf{E}'' : as can be seen from Eqs. (34), (35) and (36), the electric field is present within the ion conservation equation only through the convection terms, which depend on \mathbf{E}'' . It follows that the ion conservation equation is independent of the potential equation only when \mathbf{E}'' vanishes. For the planar front configuration, \mathbf{E}'' is essentially zero when no magnetic field is applied but becomes substantial otherwise (see Fig. 10). This obviously results in a stronger coupling at higher magnetic field, hence requiring more nodes to obtain a grid-converged

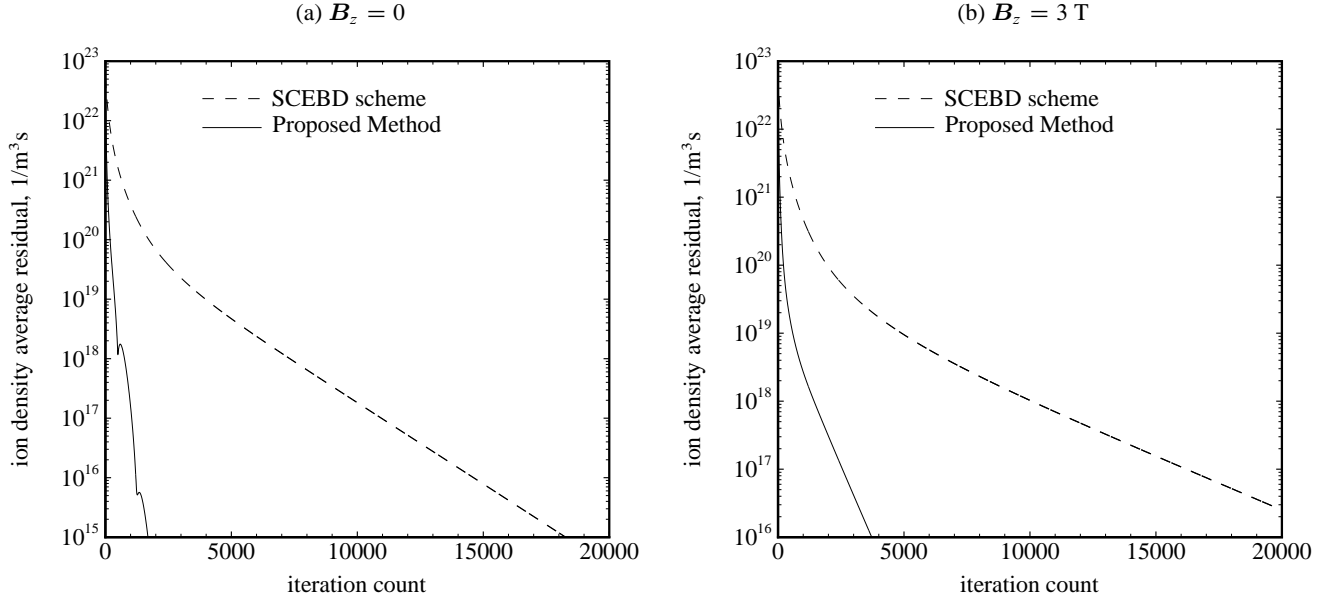


FIGURE 9. Effect of magnetic field on the residual convergence history for the planar front configuration using a grid of 200×100 nodes. In solving the ion conservation equation, the CFL number is set to the largest possible value (CFL = 4 for the proposed method and CFL = 0.5 for the SCEBD scheme) and a_{ref} is set to 300 m/s. In solving the potential equation, the characteristic length L_c is set to 1 mm.

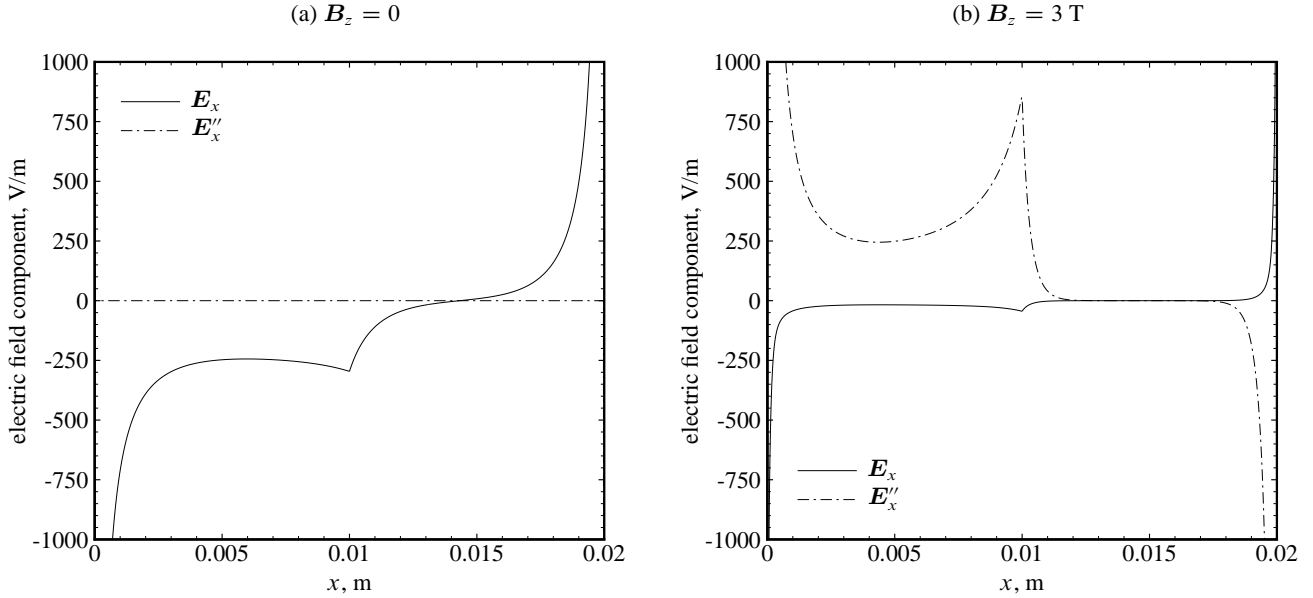


FIGURE 10. Impact of magnetic field on the components of the electric field at $y = 5 \text{ mm}$ for the planar front configuration using a mesh of 800×400 nodes.

solution.

The more substantial amount of coupling at high magnetic field also induces slower convergence, as can be seen from Fig. 9. Typically, the number of iterations needed to obtain a converged solution is increased twofold when the Hall parameter is raised from 0 to about 100. Although not shown here, a similar trend has been observed for different problem setups and different grid sizes. Also shown in Fig. 9 is a comparison of the residual convergence histories between the SCEBD scheme and the proposed method. To enable a fair comparison, both schemes use the same implicit pseudotime stepping approach based on approximate factorization. As well, the CFL number is set to as high a value as possible for each scheme, and this has been assured to yield the fastest convergence. The SCEBD scheme is seen to require 7-10 times more iterations to reach convergence than the proposed method. For a finer mesh, the difference in performance between the two methods is even

more substantial. For instance, for the finest mesh considered here (800×400 nodes), the SCEBD scheme is seen to require a computing effort 30 times greater than the proposed method. This is attributed to the ambipolar diffusion terms within the SCEBD scheme depending strongly on the electric field, hence inducing a much more substantial coupling between the ion conservation equation and the potential equation (see Appendix A for details).

7. Conclusions

A novel form of the ion flow rate is proposed for simulations of ambipolar diffusion and drift phenomena within a multicomponent plasma in the simultaneous presence of current, of an electric field, and of a magnetic field. The proposed method is superior to alternative approaches in two ways: (i) it is derived from the physical model without introducing *ad hoc* approximate weighting factors or making any other approximation and (ii) it reduces the dependence of the ion conservation equation on the potential equation by recasting the ion conservation equation in terms of drift and ambipolar diffusion components, with the latter not being dependent on the electric field. This alleviates the stiffness of the system of equations and reduces the number of iterations to reach convergence by a factor of 10 or more.

Several test cases are considered in which the recast ion conservation equation is solved in conjunction with a form of the potential equation obtained from the generalized Ohm’s law. Specifically, numerical results are obtained for 1D unsteady problems of ambipolar diffusion and drift in a multicomponent plasma, and 2D steady problems of ambipolar diffusion in the presence of a strong magnetic field. The results obtained indicate that considerably fewer grid points are needed to capture ambipolar diffusion in the absence of an applied electric field or magnetic field. This is verified not to be due to a change in the order of accuracy of the method, which remains close to 2 whether or not a strong field is applied. Rather, this is due to the decreased coupling between the ion conservation equation and the potential equation in the absence of an applied field. Either in the presence or absence of a strong applied field, the rate of convergence of the proposed method is observed to be several times higher than the one obtained using alternative approaches.

What makes the ion flow rate formulation proposed herein particularly appealing is that (i) it yields much faster convergence without affecting the accuracy of the converged solution and (ii) it is not restricted to specific discretization or relaxation schemes and can hence be readily implemented in existing flow solvers. Because it is developed in general form, the proposed method is applicable to a multicomponent plasma in the simultaneous presence of electric current and of electric and magnetic fields. The method is hence notably well-suited to simulate ambipolar diffusion within ionized multi-species flow solvers and is recommended for all flowfields as long as the plasma remains weakly-ionized and quasi-neutral.

Acknowledgment

This work was supported for one year by a Pusan National University Research Grant, 2008.

A. SCEBD Ambipolar Diffusion Model

One method that can be used to predict the ambipolar diffusion phenomenon in a multicomponent plasma under the influence of a magnetic field is the so-called Self-Consistent Effective Binary Diffusion Approximation (SCEBD) scheme proposed by Ramshaw and Shang [22, 23, 24] as implemented in Ref. [25]. The SCEBD scheme consists of solving the following conservation equation for each type of ions:

$$\frac{\partial N_k}{\partial t} + \sum_{i=1}^3 \frac{\partial}{\partial x_i} N_k V_i^n - \sum_{i=1}^3 \frac{\partial}{\partial x_i} \left(\frac{D_k^{\text{eff}}}{m_k R_k T_k} \mathbf{G}_i^k - \sum_{r \neq k}^e \frac{c_k D_r^{\text{eff}}}{m_k R_r T_r} \mathbf{G}_i^r \right) = W_k \quad (\text{A.1})$$

where V^n is the velocity of the neutrals, c_k the mass fraction, m_k the molecular mass, \mathcal{M}_k the molecular weight, W_k the chemical reaction source term, and R_k the gas constant equal to $\mathcal{R}/\mathcal{M}_k$ with \mathcal{R} the universal gas constant. The effective binary diffusivity of the ions is set to:

$$D_k^{\text{eff}} = \left(1 - \frac{\omega_k}{\sum_r \omega_r} \right) \bigg/ \sum_{r \neq k, e} \frac{P_r}{D_{kr} P} \quad (\text{A.2})$$

where P_r is the partial pressure, P is the bulk pressure, D_{kr} is the diffusivity of species k into species r , and ω_k is the “weighting factor” selected as $\omega_k \approx \rho_k / \sqrt{\mathcal{M}_k}$. In determining the effective diffusivity, an expression for the “driving force” \mathbf{G} is required:

$$\mathbf{G}^k = -N_k C_k (\mathbf{E} + \mathbf{V}^k \times \mathbf{B}) + c_k \mathbf{J} \times \mathbf{B} + \mathbf{H}^k \quad (\text{A.3})$$

where, in the case of no thermal diffusion, H^k corresponds to:

$$\mathbf{H}^k = \nabla P_k - c_k \nabla P \quad (\text{A.4})$$

A.1. SCEBD Scheme for a Three-Component Weakly-Ionized Plasma

For a three-component plasma (one type of positive ions, electrons, and neutrals), the effective diffusivity of the ions becomes:

$$D_i^{\text{eff}} = \left(1 - \frac{\omega_i}{\omega_i + \omega_e + \omega_n}\right) \bigg/ \frac{P_n}{D_{\text{in}} P} \quad (\text{A.5})$$

In the limit of a weakly-ionized plasma, it can be shown that $\omega_i \ll \omega_n$, that $\omega_e \ll \omega_n$, and that $P_n = P$. Then, the ions effective diffusivity becomes:

$$D_i^{\text{eff}} = D_{\text{in}} \quad (\text{A.6})$$

Using similar arguments, it can also be demonstrated that the neutrals effective diffusivity collapses to:

$$D_n^{\text{eff}} = D_{\text{in}} \quad (\text{A.7})$$

Then, after substituting the ion and neutral effective diffusivities back in the ion conservation equation (A.1), and assuming that (i) the plasma is weakly-ionized (i.e. $c_i \ll 1$), (ii) the mass of the ions is equal to the one of the neutrals ($m_i = m_n$), (iii) the ion gas constant is equal to the neutrals gas constant ($R_i = R_n$), and (iv) the ion temperature is equal to the one of the neutrals ($T_i = T_n$), we obtain:

$$\frac{\partial N_i}{\partial t} + \sum_{i=1}^3 \frac{\partial}{\partial x_i} N_i V_i^n - \sum_{i=1}^3 \frac{\partial}{\partial x_i} \frac{D_{\text{in}} (G_i^i - c_i G_i^n)}{m_i R_i T_i} = W_i \quad (\text{A.8})$$

In the absence of thermal diffusion, and assuming that the plasma is weakly-ionized (i.e. $c_i \ll 1$), the terms function of the “driving force” can be shown to collapse to:

$$\mathbf{G}^i - c_i \mathbf{G}^n = -N_i C_i (\mathbf{E} + \mathbf{V}^i \times \mathbf{B}) + \nabla P_i \quad (\text{A.9})$$

After substituting the latter in the ion conservation equation A.8, the following is obtained:

$$\frac{\partial N_i}{\partial t} + \sum_{i=1}^3 \frac{\partial}{\partial x_i} N_i V_i^n - \sum_{i=1}^3 \frac{\partial}{\partial x_i} \frac{D_{\text{in}} (-N_i C_i (\mathbf{E} + \mathbf{V}^i \times \mathbf{B})_i + \nabla_i P_i)}{m_i R_i T_i} = W_i \quad (\text{A.10})$$

Then, after expressing the diffusivity in terms of the mobility using the Einstein-Smoluchowski relation $D_{\text{in}} = \mu_i k_B T_i / |C_i|$, and noting that $R_i = k_B / m_i$ and that $C_i = |C_i|$, we obtain the SCEBD scheme for a three-component weakly-ionized plasma:

$$\frac{\partial N_i}{\partial t} + \sum_{i=1}^3 \frac{\partial}{\partial x_i} N_i V_i^n - \underbrace{\sum_{i=1}^3 \frac{\partial}{\partial x_i} (-\mu_i N_i (\mathbf{E} + \mathbf{V}^i \times \mathbf{B})_i)}_{\text{ambipolar diffusion and drift terms}} - \underbrace{\sum_{i=1}^3 \frac{\partial}{\partial x_i} \left(\frac{\mu_i}{|C_i|} \frac{\partial P_i}{\partial x_i} \right)}_{\text{molecular diffusion terms}} = W_i \quad (\text{A.11})$$

The latter equation shows clearly that the SCEBD scheme yields no advantage over the original form of the ion conservation outlined in Eq. (3) with the ion velocity determined from Eq. (4). That is, the ambipolar diffusion terms in the SCEBD scheme are strongly dependent on the electric field. This results in a strong coupling between the ion conservation equation and the potential equation, and makes the SCEBD scheme difficult (or even impossible) to integrate for many problems in which the electric field is determined through the generalized Ohm’s law.

B. Theoretical Expressions of Ambipolar Diffusion in a Magnetic Field

In this section, some expressions are derived for the ambipolar diffusion coefficient in the presence of a magnetic field starting from the physical model outlined in Section 2. An expression is first derived for the case of negligible transverse electric field (i.e. “classical theory”). This is followed by a derivation of the ambipolar diffusion coefficient for the case of negligible transverse current.

B.1. Ambipolar Diffusion for Negligible Transverse Electric Field (Classical Theory)

Consider a diffusion wave proceeding along x , with the magnetic field oriented along z . Then, Eq. (6) yields the following velocity for the charged species:

$$\mathbf{V}_x^k = \frac{s_k \mu_k}{1 + \mu_k^2 B_z^2} (\mathbf{E}_x + s_k \mu_k B_z \mathbf{E}_y) - \frac{\mu_k}{(1 + \mu_k^2 B_z^2) |C_k| N_k} \left(\frac{\partial P_k}{\partial x} + s_k \mu_k B_z \frac{\partial P_k}{\partial y} \right) \quad (\text{B.1})$$

Further consider a problem configuration that is such that the component of the electric field perpendicular to the diffusion wave is zero:

$$\mathbf{E}_y = 0 \quad (\text{B.2})$$

Because the x -axis is parallel to the diffusion wave, there is no density gradient of the charged species along y . Then, assuming that the temperature gradients yield negligible changes in the charged species velocity, Eq. (B.1) yields the following electron and ion velocities:

$$\mathbf{V}_x^e = -\frac{\mu_e}{1 + \mu_e^2 B_z^2} \mathbf{E}_x - \frac{\mu_e k_B T_e}{(1 + \mu_e^2 B_z^2) |C_e| N_e} \frac{\partial N_e}{\partial x} \quad (\text{B.3})$$

$$\mathbf{V}_x^i = \frac{\mu_i}{1 + \mu_i^2 B_z^2} \mathbf{E}_x - \frac{\mu_i k_B T_i}{(1 + \mu_i^2 B_z^2) |C_i| N_i} \frac{\partial N_i}{\partial x} \quad (\text{B.4})$$

After multiplying and adding the latter two equations in such a way as to eliminate the electric field, and further assuming that the plasma is neutral and that there is no current flowing parallel to the diffusion wave (*i.e.* $\mathbf{V}_x^e = \mathbf{V}_x^i$), it is easy to show that the ion flow rate is equal to:

$$N_i \mathbf{V}_x^i = -D_a \frac{\partial N_i}{\partial x} \quad (\text{B.5})$$

with the ambipolar diffusion coefficient equal to:

$$D_a = \frac{\mu_i \mu_e k_B (T_e + T_i)}{\mu_i |C_i| (1 + \mu_e^2 B_z^2) + \mu_e |C_e| (1 + \mu_i^2 B_z^2)} \quad (\text{B.6})$$

Then, noting that $\mu_i \ll \mu_e$, and using the Einstein-Smoluchowski relation $D_i = \mu_i k_B T_i / |C_i|$, the latter can be easily shown to collapse to:

$$D_a = \frac{D_i}{1 + \mu_i \mu_e B_z^2} \left(1 + \frac{T_e}{T_i} \right) \quad (\text{B.7})$$

As can be seen from this derivation, the physical model used herein does collapse to the classical theory of ambipolar diffusion in the presence of magnetic field. The classical theory assumes, however, that the diffusion proceeds under zero transverse electric field.

B.2. Ambipolar Diffusion for Negligible Transverse Current

In this section, an expression is derived for the ambipolar diffusion coefficient when the transverse electric field is such that the transverse current vanishes. This can be done starting from the physical model outlined in Section 2 and going through the same steps as when deriving the classical expression [see Eqs. (B.1) to (B.7)], but assuming zero transverse current instead of zero transverse electric field. For this purpose, consider a diffusion wave proceeding along x , with the magnetic field oriented along z . Then, the velocity of the charged species (either electrons or ions) can be found from Eq. (6):

$$\mathbf{V}_x^k = \frac{s_k \mu_k}{1 + \mu_k^2 B_z^2} (\mathbf{E}_x + s_k \mu_k B_z \mathbf{E}_y) - \frac{\mu_k}{(1 + \mu_k^2 B_z^2) |C_k| N_k} \left(\frac{\partial P_k}{\partial x} + s_k \mu_k B_z \frac{\partial P_k}{\partial y} \right) \quad (\text{B.8})$$

Because the x -axis is parallel to the diffusion wave, there is no density gradient of the charged species along y . Then, disregarding the temperature gradients, Eq. (B.8) yields the following charged species velocity:

$$\mathbf{V}_x^k = \frac{s_k \mu_k}{1 + \mu_k^2 B_z^2} (\mathbf{E}_x + s_k \mu_k B_z \mathbf{E}_y) - \frac{\mu_k k_B T_k}{(1 + \mu_k^2 B_z^2) |C_k| N_k} \frac{\partial N_k}{\partial x} \quad (\text{B.9})$$

Now, it is desired to find \mathbf{E}_y such that the current is zero along y . This can be done starting from the vector form of the charged species velocity equation, Eq. (4), and neglecting the pressure gradient along y for the reasons mentioned above:

$$\mathbf{V}_y^k = s_k \mu_k (\mathbf{E}_y - \mathbf{V}_x^k B_z) \quad (\text{B.10})$$

Then, noting that the transverse current corresponds to $\mathbf{J}_y = \sum_k N_k C_k \mathbf{V}_y^k$, it follows that:

$$\mathbf{J}_y = -\mu_e C_e N_e (\mathbf{E}_y - \mathbf{V}_x^e B_z) + \mu_i C_i N_i (\mathbf{E}_y - \mathbf{V}_x^i B_z) \quad (\text{B.11})$$

The latter is now set to zero to obtain the condition corresponding to zero transverse current:

$$\mathbf{J}_y = 0 \quad (\text{B.12})$$

Substituting Eq. (B.12) into (B.11), and assuming a neutral plasma and also assuming no current parallel to the diffusion process (*i.e.* $\mathbf{V}_x^e = \mathbf{V}_x^i$), it can be easily shown that the electric field transverse to the diffusion is equal to:

$$\mathbf{E}_y = \mathbf{V}_x^e B_z = \mathbf{V}_x^i B_z \quad (\text{B.13})$$

Then, after substituting Eq. (B.13) into Eq. (B.9), we obtain the electron and ion velocities parallel to the diffusion wave:

$$\mathbf{V}_x^e = -\mu_e \mathbf{E}_x - \frac{\mu_e k_B T_e}{|C_e| N_e} \frac{\partial N_e}{\partial x} \quad (\text{B.14})$$

$$\mathbf{V}_x^i = \mu_i \mathbf{E}_x - \frac{\mu_i k_B T_i}{|C_i| N_i} \frac{\partial N_i}{\partial x} \quad (\text{B.15})$$

After multiplying and adding the latter two equations in such a way as to eliminate the electric field, and further assuming that the plasma is neutral and that there is no current flowing parallel to the diffusion wave (*i.e.* $\mathbf{V}_x^e = \mathbf{V}_x^i$), it is easy to show that the ion flow rate is equal to:

$$N_i \mathbf{V}_x^i = -D_a \frac{\partial N_i}{\partial x} \quad (\text{B.16})$$

with the ambipolar diffusion coefficient equal to:

$$D_a = \frac{\mu_i \mu_e k_B (T_e + T_i)}{|C_i| (\mu_i + \mu_e)} \quad (\text{B.17})$$

Then, noting that the mobility of the ions is much lower than the one of the electrons and using the Einstein-Smoluchowski relation, the latter becomes:

$$D_a = D_i \left(1 + \frac{T_e}{T_i} \right) \quad (\text{B.18})$$

The ambipolar diffusion coefficient for a plasma with the charge carriers limited to electrons and one type of positive ions is seen here not to be dependent directly on the magnetic field when the transverse current is zero. A comparison of Eq. (B.18) to the previously derived classical ambipolar diffusion coefficient in Eq. (B.7) reveals the profound difference that the transverse electric field has on the ambipolar diffusion coefficient. When the transverse electric field is zero, the ambipolar diffusion coefficient is inversely proportional to the square of the magnetic field, as given by the classical theory. In contrast, should the transverse electric field be non-zero and such that it results in no transverse current, the ambipolar diffusion coefficient would be unaffected by the magnetic field.

References

- [1] HOLT, E. H. AND HASKELL, R. E., *Foundations of Plasma Dynamics*, MacMillan Company, New-York, 2nd ed., 1965.
- [2] HUANG, P. G., SHANG, J. S., AND STANFIELD, S. A., "Periodic Electrodynamics Field of Dielectric Barrier Discharge," *AIAA Journal*, Vol. 49, No. 1, 2011, pp. 119.
- [3] BISEK, N. J., BOYD, I. D., AND POGGIE, J., "Numerical Study of Plasma-Assisted Aerodynamic Control for Hypersonic Vehicles," *Journal of Spacecraft and Rockets*, Vol. 46, No. 3, 2009, pp. 568.
- [4] LINDSEY, M., GAITONDE, D., AND CAMBEROS, J., "Computational Study of Magnetogasdynamic Inlet Flow Control on a Flight-Scale Scramjet," *AIAA Journal*, Vol. 45, No. 6, 2007, pp. 1258–1269.
- [5] WAN, T., CANDLER, G. V., MACHERET, S. O., AND SHNEIDER, M. N., "Three-Dimensional Simulation of the Electric Field and Magnetohydrodynamic Power Generation During Reentry," *AIAA Journal*, Vol. 47, No. 6, 2009, pp. 1327.
- [6] PARENT, B., MACHERET, S., SHNEIDER, M., AND HARADA, N., "Numerical Study of an Electron-Beam-Confined Faraday Accelerator," *Journal of Propulsion and Power*, Vol. 23, No. 5, 2007, pp. 1023–1032.
- [7] THOMPSON, J. B., "Negative Ions in the Positive Column of the Oxygen Discharge," *Proceedings of the Physical Society*, Vol. 73, No. 5, 1959, pp. 818–820.
- [8] OSKAM, H. J., *Philips Research Report*, Vol. 13, 1958, pp. 335.

- [9] SUSLOV, O. N. AND TIRSKII, G. A., "Definition and Calculation of Effective Ambipolar Diffusion Coefficients for a Laminar Multicomponent Ionized Boundary Layer," *Journal of Applied Mechanics and Technical Physics*, Vol. 11, No. 4, 1970, pp. 575–584.
- [10] ROGOFF, G. L., "Ambipolar Diffusion Coefficients for Discharges in Attaching Gases," *Journal of Physics D: Applied Physics*, Vol. 18, 1985, pp. 1533–1545.
- [11] RAMSHAW, J. D. AND CHANG, C. H., "Ambipolar Diffusion in Multicomponent Plasmas," *Plasma Chemistry and Plasma Processing*, Vol. 11, No. 3, 1991, pp. 395–402.
- [12] RAMSHAW, J. D. AND CHANG, C. H., "Ambipolar Diffusion in Two-Temperature Multicomponent Plasmas," *Plasma Chemistry and Plasma Processing*, Vol. 13, No. 3, 1993, pp. 489–498.
- [13] HOH, F. C., "Low-Temperature Plasma Diffusion in a Magnetic Field," *Review of Modern Physics*, Vol. 34, No. 2, 1962, pp. 267–286.
- [14] FREDRICKS, R. W. AND MASTRUP, F., "Ambipolar Diffusion of a Plasma in a Weak Magnetic Field," *The Physics of Fluids*, Vol. 6, No. 1, 1963, pp. 36–39.
- [15] MALDONADO, C. D., "Ambipolar Diffusion and Drift of Added Carriers in a Semiconductor in the Presence of a Magnetic Field," *Journal of Plasma Physics*, Vol. 1, No. 1, 1967, pp. 113–128.
- [16] CHMIELESKI, R. M. AND FERZIGER, J. H., "Transport Properties of a Nonequilibrium Partially Ionized Gas in a Magnetic Field," *The Physics of Fluids*, Vol. 10, No. 12, 1967, pp. 2520–2530.
- [17] DEVOTO, R. S., "Heat and Diffusion Fluxes in a Multicomponent Ionized Gas in a Magnetic Field. I. General Expressions," *Z. Naturforsch.*, Vol. 24a, 1969, pp. 967–976.
- [18] DAYBELGE, U., "Unified Transport Theory of Partially Ionized Nonisothermal Plasmas," *Journal of Applied Physics*, Vol. 41, 1970, pp. 2130–2139.
- [19] ROZHANSKY, V. A. AND TSENDIN, L. D., *Transport Phenomena in Partially Ionized Plasma*, Taylor and Francis, New-York, NY, 2001.
- [20] PEERENBOOM, K. S. C., VAN DIJK, J., GOEDHEER, W. J., AND VANDER MULLEN, J. J. A. M., "On the Ambipolar Constraint in Multi-Component Diffusion Problems," *Journal of Computational Physics*, Vol. 230, 2011, pp. 3651–3655.
- [21] PEERENBOOM, K. S. C., VAN DIJK, J., GOEDHEER, W. J., DEGREZ, G., AND VANDER MULLEN, J. J. A. M., "A Finite Volume Model for Multi-Component Diffusion in Magnetically Confined Plasmas," *Journal of Physics D*, Vol. 44, 2011, pp. 1–8.
- [22] RAMSHAW, J. D. AND CHANG, C. H., "Multicomponent Diffusion in Two-Temperature Magnetohydrodynamics," *Physical Review E*, Vol. 53, No. 6, 1996, pp. 6382–6388.
- [23] RAMSHAW, J. D. AND CHANG, C. H., "Friction-Weighted Self-Consistent Effective Binary Diffusion Approximation," *Journal of Non-Equilibrium Thermodynamics*, Vol. 21, 1996, pp. 223–232.
- [24] RAMSHAW, J. D., "Self-Consistent Effective Binary Interaction Approximation for Strongly Coupled Multifluid Dynamics," *Journal of Non-Equilibrium Thermodynamics*, Vol. 23, No. 2, 1998, pp. 135–140.
- [25] PARK, J., HEBERLEIN, J., PFENDER, E., CANDLER, G., AND CHANG, C. H., "Two-Dimensional Numerical Modeling of Direct-Current Electric Arcs in Nonequilibrium," *Plasma Chemistry and Plasma Processing*, Vol. 28, 2008, pp. 213–231.
- [26] PARENT, B., SHNEIDER, M. N., AND MACHERET, S. O., "Generalized Ohm's Law and Potential Equation in Computational Weakly-Ionized Plasmadynamics," *Journal of Computational Physics*, Vol. 230, No. 4, 2011, pp. 1439–1453.
- [27] YEE, H. C., KLOPPER, G. H., AND MONTAGNÉ, J.-L., "High-Resolution Shock-Capturing Schemes for Inviscid and Viscous Hypersonic Flows," *Journal of Computational Physics*, Vol. 88, 1990, pp. 31–61.
- [28] PEACEMAN, D. W. AND RACHFORD, H. H., "The Numerical Solution of Parabolic and Elliptic Differential Equations," *Journal of the Society of Industrial and Applied Mathematics*, Vol. 3, 1955, pp. 28–41.
- [29] SINNOT, G., GOLDEN, D. E., AND VARNEY, R. N., "Positive-Ion Mobilities in Dry Air," *Physical Review*, Vol. 170, No. 1, 1968, pp. 272–275.
- [30] GOSHO, Y. AND HARADA, A., "A New Technique for Measuring Negative Ion Mobilities at Atmospheric Pressure," *Journal of Physics D*, Vol. 16, 1983, pp. 1159–1166.
- [31] GRIGORIEV, I. S. AND MEILIKHOV, E. Z., *Handbook of Physical Quantities*, CRC, Boca Raton, Florida, 1997.
- [32] RAIZER, Y. P., *Gas Discharge Physics*, Springer-Verlag, Berlin, Germany, 1991.
- [33] KOSSYI, A., KOSTINSKY, A. Y., MATVEYEV, A. A., AND SILAKOV, V. P., "Kinetic Scheme of the Non-Equilibrium Discharge in Nitrogen-Oxygen Mixtures," *Plasma Sources Science and Technology*, Vol. 1, 1992, pp. 207–220.
- [34] PETERSON, L. R. AND GREEN, A. E. S., "The Relation Between Ionization Yields, Cross Sections, and Loss Functions," *Journal of Physics B: Atomic, Molecular and Optical Physics*, Vol. 1, No. 6, 1968, pp. 1131–1140.